JB
Journals.ASM.org

A Trigger Residue for Transmembrane Signaling in the *Escherichia coli* Serine Chemoreceptor

Smiljka Kitanovic, Peter Ames, John S. Parkinson
Biology Department, University of Utah, Salt Lake City, Utah, USA

ABSTRACT

The transmembrane Tsr protein of *Escherichia coli* mediates chemotactic responses to environmental serine gradients. Serine binds to the periplasmic domain of the homodimeric Tsr molecule, promoting a small inward displacement of one transmembrane helix (TM2). TM2 piston displacements, in turn, modulate the structural stability of the Tsr-HAMP domain on the cytoplasmic side of the membrane to control the autophosphorylation activity of the signaling CheA kinase bound to the membrane-distal cytoplasmic tip of Tsr. A five-residue control cable segment connects TM2 to the AS1 helix of HAMP and transmits stimulus and sensory adaptation signals between them. To explore the possible role of control cable helicity in transmembrane signaling by Tsr, we characterized the signaling properties of mutant receptors with various control cable alterations. An all-alanine control cable shifted Tsr output toward the kinase-on state, whereas an all-glycine control cable prevented Tsr from reaching either a fully on or fully off output state. Restoration of the native isoleucine (I214) in these synthetic control cables largely alleviated their signaling defects. Single amino acid replacements at Tsr-I214 shifted output toward the kinase-off (L, N, H, and R) or kinase-on (A and G) states, whereas other control cable residues tolerated most amino acid replacements with little change in signaling behavior. These findings indicate that changes in control cable helicity might mediate transitions between the kinase-on and kinase-off states during transmembrane signaling by chemoreceptors. Moreover, the Tsr-I214 side chain plays a key role, possibly through interaction with the membrane interfacial environment, in triggering signaling changes in response to TM2 piston displacements.

IMPORTANCE

The Tsr protein of *E. coli* mediates chemotactic responses to environmental serine gradients. Stimulus signals from the Tsr periplasmic sensing domain reach its cytoplasmic kinase control domain through piston displacements of a membrane-spanning helix and an adjoining five-residue control cable segment. We characterized the signaling properties of Tsr variants to elucidate the transmembrane signaling role of the control cable, an element present in many microbial sensory proteins. Both the kinase-on and kinase-off output states of Tsr depended on control cable helicity, but only one residue, I214, was critical for triggering responses to attractant inputs. These findings suggest that signal transmission in Tsr involves modulation of control cable helicity through interaction of the I214 side chain with the cytoplasmic membrane.

The receptor proteins that mediate chemotactic behaviors in motile bacteria offer powerful experimental models for investigating transmembrane signaling mechanisms. The aspartate/maltose (Tar) and serine (Tsr) chemoreceptors of *Escherichia coli*, members of the superfamily of methyl-accepting chemotaxis proteins (MCPs), have been studied most extensively in this regard (reviewed in reference 1). Both operate as membrane-spanning homodimers (Fig. 1), with a periplasmic ligand-binding domain that monitors chemoeffector levels in the environment and a cytoplasmic kinase control domain that communicates with the cell's flagellar motors through a phosphorelay signaling pathway. The MCP kinase control domain forms stable signaling complexes with two cytoplasmic proteins: CheA, a histidine autokinase, and CheW, which couples CheA autophosphorylation activity to receptor control. CheA donates phosphoryl groups to the CheY response regulator to govern the cell's swimming behavior. The flagellar motors rotate counterclockwise by default, producing forward swimming. Phospho-CheY enhances clockwise motor rotation, which causes random changes in swimming direction.

Receptor signaling complexes modulate CheA activity in response to ligand occupancy changes. Unliganded receptors activate CheA, whereas attractant-bound receptors deactivate CheA. Following a stimulus-induced kinase control response, receptor molecules undergo reversible modifications at sensory adaptation sites near the kinase control domain (Fig. 1). Glutamate (E) residues at the adaptation sites favor a kinase-off (OFF) output state, whereas glutamyl methyl esters (Em), or glutamine residues, which mimic methylated sites, favor a kinase-on (ON) signaling state. Receptors in the kinase-off signaling state are good substrates for CheR, an MCP-specfic methyltransferase; receptors in the kinase-on signaling state are good substrates for CheB, an MCP-specific methylesterase and deamidase (Fig. 1B). Adapta-

Received 8 April 2015 **Accepted** 18 May 2015
Accepted manuscript posted online 26 May 2015
Citation Kitanovic S, Ames P, Parkinson JS. 2015. A trigger residue for transmembrane signaling in the *Escherichia coli* serine chemoreceptor. J Bacteriol 197:2568–2579. doi:10.1128/JB.00274-15.
Editor: A. M. Stock
Address correspondence to John S. Parkinson, parkinson@biology.utah.edu.
Supplemental material for this article may be found at http://dx.doi.org/10.1128/JB.00274-15.

doi:10.1128/JB.00274-15

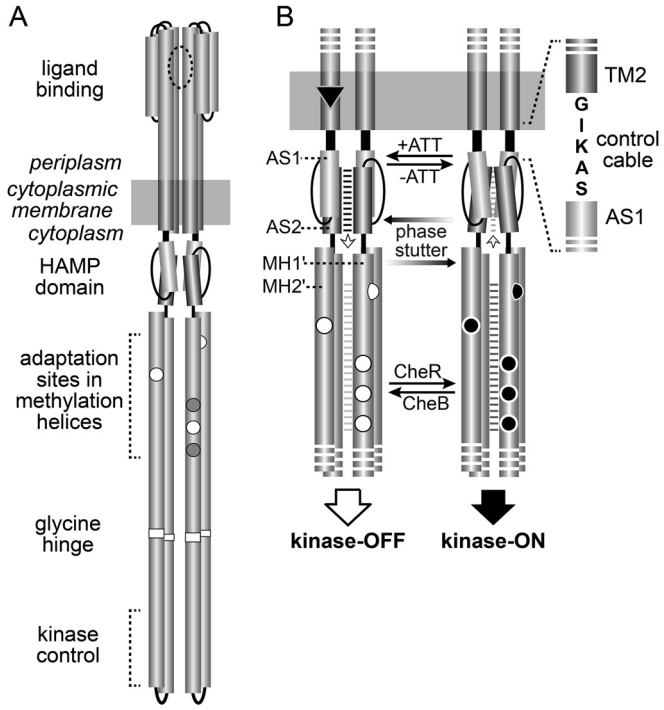

FIG 1 Tsr structural elements involved in transmembrane signaling. (A) The Tsr homodimer. Cylindrical segments represent α-helices, drawn approximately to scale. Each Tsr subunit has five adaptation sites: white circles represent E residues capable of accepting methyl groups; gray circles represent Q residues that must be deamidated by CheB before they can be methylated by CheR. (B) Dynamic-bundle model of Tsr-HAMP signaling. AS1 and AS2 are helices from one subunit in the four-helix HAMP bundle; MH1′ and MH2′ are helices from one subunit in the four-helix methylation bundle. The model proposes that packing stabilities of the HAMP and MH bundles are coupled in opposition by the phase stutter arrangement that joins the AS2 and MH1 helices (7). Unmethylated adaptation sites (white circles) destabilize the MH bundle, which promotes HAMP packing. Methylated sites (black circles) stabilize the MH bundle, which reduces HAMP packing. The HAMP-MH interplay poises the two bundles for stimulus responses: attractants enhance HAMP stability; repellents reduce HAMP stability. These stimulus signals are transmitted to the AS1 helices of HAMP through the TM2 transmembrane helices and the intervening control cable residues.

tional modifications offset receptor signaling shifts to restore prestimulus CheA kinase activity, enabling a swimming cell to detect relatively small changes in chemoeffector concentration over a wide concentration range.

Tar and Tsr molecules have two symmetric, negatively cooperative ligand-binding sites at the dimer interface of their periplasmic domains (Fig. 1A). Ligand occupancy at one binding site promotes two asymmetric conformational changes in these receptor molecules. (i) A rotational reorientation of the two subunits partly closes the unoccupied binding site and is most likely responsible for negative cooperativity at the second binding site (2). Molecular dynamics simulations indicate that the ligand-induced subunit rotation does not propagate structural changes to the transmembrane helices, and therefore, it seems unlikely that it contributes directly to stimulus control of receptor output (2). (ii) Ligand binding also produces a small (~2 Å) inward displacement of one transmembrane helix (TM2) (3–5) (Fig. 1B). The stimulus-induced piston movement of TM2 promotes conformational changes in other parts of the receptor molecule that shift it to a kinase-off signaling state. A HAMP domain at the cytoplasmic end of TM2 plays a key role in these signaling transactions (6) (Fig. 1B).

The dynamic-bundle model of HAMP signaling (6, 7) proposes that the packing stability of the HAMP domain, a four-helix bundle, opposes that of the four-helix methylation bundle through a phase-stutter connection (Fig. 1B). Attractant stimuli stabilize HAMP and destabilize the methylation helix (MH) bundle; adaptational modifications enhance MH packing and reduce HAMP stability. The packing stabilities of the MH bundle and kinase control tip of the receptor molecule also appear to be coupled in yin-yang fashion (8) through an intervening glycine hinge region (9, 10). Thus, ligand binding to the periplasmic sensing domain produces activity changes in the CheA kinase at the cytoplasmic hairpin tip through opposed dynamic shifts in structurally coupled signaling elements of the receptor (1).

A five-residue control cable segment at the cytoplasmic end of TM2 transmits piston displacement signals to the AS1 helix of the HAMP bundle (Fig. 1B). The mechanism of signal transmission through the control cable is not well understood, but mutational analyses (11, 12) and molecular dynamics studies (13, 14) indicate that an α-helical secondary structure could be important for control cable function. In the present study, we tested that proposition by characterizing the signaling behaviors of mutant Tsr receptors with altered control cables. These studies revealed that control cable helicity plays a role in enabling the receptor to adopt both kinase-on and kinase-off output states, but only one control cable residue, I214, is critical to the transmission mechanism. The signaling properties of mutant control cables with various amino acid replacements at this key position suggest that changes in control cable helicity play a key role in transmembrane signaling. This insight enabled us to devise an explicit mechanistic model for transmembrane signaling by Tsr.

MATERIALS AND METHODS

Bacterial strains. Strains used in this study were isogenic derivatives of *E. coli* K-12 strain RP437 (15). Their designations and relevant genotypes (in brackets) are as follows: UU1250 [Δ*aer-1* Δ*tsr-7028* Δ(*tar-tap*)*5201* Δ*trg-100*] (16), UU2610 [Δ*aer-1* Δ(*tar-cheB*)*4346* Δ*tsr-5547* Δ*trg-4543*] (17), UU2611 [Δ*aer-1* Δ(*tar-cheR*)*4283* Δ*tsr-5547* Δ*trg-4543*] (17), UU2612 [Δ*aer-1* Δ(*tar-tap*)*4530* Δ*tsr-5547* Δ*trg-4543*] (17), UU2632 [Δ*aer-1* Δ(*tar-tap*)*4530* Δ(*cheB*)*4345* Δ*tsr-5547* Δ*trg-4543*] (17), UU2567 [Δ(*tar-cheZ*)*4211* Δ(*tsr*)*-5547* Δ(*aer*)*-1* Δ*trg-4543*] (18), UU2697 [Δ(*cheY-cheZ*)*1215* Δ(*cheB*)*4345* Δ(*tar-tap*)*4530* Δ*tsr-5547* Δ*aer-1* Δ*trg-4543*] (18), UU2699 [Δ(*cheY-cheZ*)*1215* Δ(*tar-cheR*)*4283* Δ*tsr-5547* Δ*aer-1* Δ*trg-4543*] (18), and UU2700 [Δ(*cheY-cheZ*)*1215* Δ(*tar-tap*)*4530* Δ*tsr-5547* Δ*aer-1* Δ*trg-4543*] (18).

CheR and CheB phenotype notation. A shorthand notation is used throughout to indicate strain phenotypes with respect to the CheR (R^- and R^+) and CheB (B^- and B^+) proteins.

Plasmids. Plasmids used in the study were pKG116, a derivative of pACYC184 (19) that confers chloramphenicol resistance and has a sodium salicylate-inducible expression/cloning site (20); pPA114, a relative of pKG116 that carries wild-type *tsr* under salicylate control (16); pRZ30, a derivative of pKG116 that expresses CheY-YFP and CheZ-CFP fusion proteins under salicylate control (18); pRR48, a derivative of pBR322 (21) that confers ampicillin resistance and has an expression/cloning site with a *tac* promoter and an ideal (perfectly palindromic) *lac* operator under the control of a plasmid-encoded *lacI* repressor, inducible by isopropyl-β-D-thiogalactopyranoside (IPTG) (22); pRR53, a derivative of pRR48 that carries wild-type *tsr* under IPTG control (22); and pVS88, a plasmid that

expresses CheY-YFP and CheZ-CFP fusion proteins under IPTG control (23).

Chemotaxis assays. Host strains carrying *tsr* plasmids were assessed for chemotactic ability on tryptone or minimal glycerol plus serine soft agar plates (24) containing the appropriate antibiotics (ampicillin [50 μg/ml] or chloramphenicol [12.5 μg/ml]) and inducers (100 μM IPTG or 0.6 μM sodium salicylate). Tryptone plates were incubated at 30 to 32.5°C for 7 to 10 h or at 24°C for 15 to 20 h. Minimal plates were incubated at 30 to 32.5°C for 15 to 20 h.

Mutant construction. Mutations in the *tsr* gene of plasmid pPA114 or pRR53 were generated by QuikChange PCR mutagenesis, using either degenerate-codon or site-specific primers, as previously described (16). QuikChange products were introduced into strain UU1250 by $CaCl_2$ transformation and tested for the ability to support Tsr function on tryptone and minimal serine soft agar plates. Candidate plasmids were verified by sequencing the entire *tsr* coding region. All plasmid derivatives were also tested for expression of the mutant protein at normal levels, as detailed below.

Expression levels and modification patterns of mutant Tsr proteins. Cells harboring pRR53 derivatives were grown in tryptone broth containing 50 μg/ml of ampicillin and 100 μM IPTG; cells harboring pPA114 derivatives were grown in tryptone broth containing 12.5 μg/ml of chloramphenicol and 0.6 μM sodium salicylate. Expression levels of mutant proteins were determined in strain UU2610 (R^- B^-) in which receptor molecules have a uniform modification state. Strains UU2611 (R^- B^+), UU2632 (R^+ B^-), and UU2612 (R^+ B^+) were used to assess the CheR and CheB substrate properties of mutant Tsr proteins. Cells were grown at 30°C to mid-exponential phase, and 1-ml samples were pelleted by centrifugation, washed twice with KEP (10 mM KPO_4, 0.1 mM K-EDTA [pH 7.0]), and lysed by boiling in sample buffer (25). Tsr bands were resolved by electrophoresis in 11% polyacrylamide gels containing sodium dodecyl sulfate (SDS-PAGE) and visualized by immunoblotting with a polyclonal rabbit antiserum raised against Tsr residues 290 to 470 (26).

To evaluate adaptational modification responses to a serine stimulus, UU2612 cells containing plasmids were grown and prepared as described above. Washed cells were divided into two 500-μl aliquots and incubated at 30°C for 20 min, after which L-serine was added to one sample at a final concentration of 10 mM. Both samples were incubated at 30°C for an additional 30 min and then analyzed by SDS-PAGE, as described above.

***In vivo* FRET CheA kinase assay.** The experimental system, cell sample chamber, stimulus protocol, and data analysis followed the hardware, software, and methods described by Sourjik et al. (23), with minor modifications (18). Cells containing a Förster resonance energy transfer (FRET) reporter plasmid (pRZ30 or pVS88) and a compatible *tsr* expression plasmid (pRR53 or pPA114 derivative) were grown at 30°C to mid-exponential phase in tryptone broth, washed, attached to a round coverslip with polylysine, and mounted in a flow cell (27). The flow cell and all motility buffer test solutions (KEP containing 10 mM sodium lactate, 100 μM methionine, and various concentrations of serine) were maintained at 30°C throughout each experiment. Cells were illuminated at the CFP excitation wavelength and light emission detected at the CFP (FRET donor) and YFP (FRET acceptor) wavelengths with photomultipliers. The ratio of YFP to CFP photon counts reflects CheA kinase activity and changes in response to serine stimuli (23, 28). In some extended experiments, differential rates of YFP and CFP bleaching caused a slow decline in YFP/CFP values. In such cases, a linear fit of YFP/CFP versus time was used to correct for baseline drift, similar to the approach used by Meir et al. (29). Fractional changes in kinase activity versus applied serine concentrations were fitted to a multisite Hill equation, yielding two parameter values: $K_{1/2}$, the attractant concentration that inhibits 50% of the kinase activity, and the Hill coefficient, reflecting the extent of cooperativity of the response (23, 30). The overall amount of receptor-generated kinase activity was defined in each experiment as the larger of two values: the activity inhibitable by a saturating serine stimulus and the activity eliminated by treatment with 3 mM KCN, which depletes cellular levels of ATP, the phosphodonor for the CheA autophosphorylation reaction (18).

RESULTS

Synthetic Tsr control cables: GGGGG and AAAAA. To assess the possible importance of α-helical secondary structure for signal transmission by the Tsr control cable, we constructed two variants of the *tsr* expression plasmid pRR53, one with an all-glycine control cable (Tsr-GGGGG) and one with an all-alanine control cable (Tsr-AAAAA). We reasoned that if the wild-type Tsr control cable had α-helical character, the all-G control cable might have reduced helix potential, whereas the all-A control cable might have enhanced helix potential. Upon transfer of the mutant plasmids to a receptorless, adaptation-competent host (UU2612), Tsr-AAAAA mediated robust chemotactic behavior on tryptone soft agar but Tsr-GGGGG did not (Fig. 2A), demonstrating that these synthetic control cables function differently. Tests on minimal soft agar plates containing 10 and 100 μM serine showed that Tsr-AAAAA had an elevated response threshold (Fig. 2B). While wild-type Tsr mediated chemotaxis to 10 μM serine, Tsr-AAAAA produced a response only at 100 μM serine (Fig. 2B). Tsr-GGGGG could not mediate a chemotactic response at either serine concentration (Fig. 2B).

We used a FRET-based *in vivo* kinase assay (28) to determine the serine dose-response characteristics of these synthetic control cable receptors in more detail. The *in vivo* kinase assay measures FRET interactions between CFP-tagged CheZ (the FRET donor) and YFP-tagged CheY (the FRET acceptor). Phosphorylation of CheY promotes binding to its phosphatase CheZ, producing a FRET signal from the tagged proteins that reflects CheA autophosphorylation activity (23). In UU2700, a FRET reporter strain containing the CheR and CheB adaptation enzymes, wild-type Tsr showed a sensitive serine response ($K_{1/2}$, ~0.5 μM) (Fig. 2C) that mainly arises from the low modification states of the receptor molecules (18, 31). In UU2567, a FRET reporter strain that lacks CheR and CheB, wild-type Tsr subunits have a QEQEE residue pattern at their five adaptation sites. The Q residues mimic methylated glutamyl (Em) residues, imparting higher kinase activity and reduced serine sensitivity ($K_{1/2}$ ~ 19 μM for wild-type Tsr) (Fig. 2C).

It is important to note that CheA kinase activities measured in the *in vivo* FRET assay do not scale over the full range of receptor modification states and response sensitivities (18, 31, 32). Wild-type Tsr molecules with 1 to 5 Q or Em modifications per subunit produce comparably high kinase activities that represent the maximum level detectable in the assay. Mutant receptors with widely different response sensitivities can also exhibit similarly high kinase activities.

In the following, we describe the signaling behaviors of Tsr control cable mutants in terms of a two-state model that involves shifts between kinase-off (OFF) and kinase-on (ON) receptor outputs driven by input stimuli and by adaptational modifications. Thus, Tsr control cable alterations that enhance serine response sensitivity shift output toward the OFF state, whereas those that reduce serine sensitivity shift output toward the ON state. In Discussion, we argue that the signaling properties of some mutant control cables are not consistent with a simple two-state structural device for modulating receptor input-output communication.

Tsr-AAAAA exhibited high kinase activity in UU2567 (R^- B^-) (Table 1) but failed to respond to serine concentrations as high as

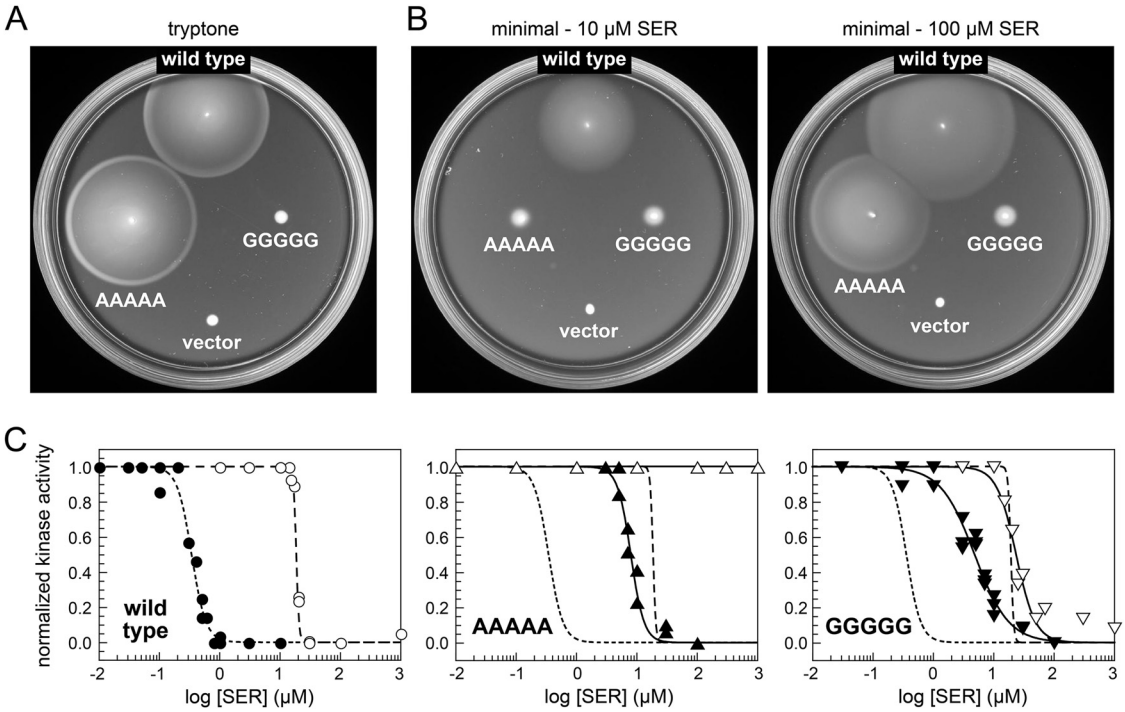

FIG 2 Signaling behaviors of Tsr synthetic control cable mutants. (A) Tryptone soft agar chemotaxis phenotypes of transducerless strain UU2612 (R^+ B^+) carrying pRR53 (wild-type Tsr) or pRR53 derivatives with an all-A or all-G control cable. The vector control is pRR48. Plates were incubated at 30°C for 8 h. (B) Minimal serine soft agar chemotaxis phenotypes of transducerless strain UU2612 (R^+ B^+) carrying pRR53 (wild-type Tsr) or pRR53 derivatives with an all-A or all-G control cable. The vector control is pRR48. Plates were incubated at 30°C for 18 h. (C) Hill fits of serine dose-response data derived from *in vivo* kinase assays of pRR53 derivatives in FRET reporter strains UU2567 (R^- B^-) (white symbols) and UU2700 (R^+ B^+) (black symbols). The curves for wild-type Tsr are reproduced in the second and third graphs without data points for comparison purposes. $K_{1/2}$ and Hill coefficient values in UU2567 and UU2700 for these particular experiments were as follows: wild-type Tsr, 19 μM and 19 (white circles) and 0.4 μM and 3.6 (black circles); Tsr-AAAAA, no response (white triangles) and 8.1 μM and 3.9 (black triangles); Tsr-GGGGG, 24 μM and 2.7 (white inverted triangles) and 4.9 μM and 1.5 (black inverted triangles).

1 mM in this reporter strain (Fig. 2C). In the adaptation-proficient UU2700 background (R^+ B^+), Tsr-AAAAA responded to serine with a threshold about 20-fold higher than that of wild-type Tsr ($K_{1/2}$, ~8 μM) (Fig. 2C). These serine response behaviors suggest that Tsr-AAAAA is shifted toward the kinase-on output state. Tsr-GGGGG, in contrast, showed serine responses in both reporter strains. In UU2567 (R^- B^-), its serine sensitivity was similar to that of wild-type Tsr ($K_{1/2}$, ~24 μM) (Fig. 2C); in UU2700 (R^+ B^+), its serine response threshold was about 10-fold higher than that of wild-type Tsr ($K_{1/2}$, ~4.9 μM) (Fig. 2C). The Tsr-GGGGG responses in both reporter strains exhibited lower cooperativities than either the Tsr-AAAAA or Tsr wild-type responses (Fig. 2C and Table 1).

Adaptation properties of Tsr-AAAAA. The different response behaviors of Tsr-AAAAA in the R^- B^- and R^+ B^+ reporter strains imply that adaptational modifications can adjust its signaling properties. To verify the ON-shifted character of Tsr-AAAAA signaling, we mutationally imposed a lower modification state (EE EQE) on this receptor, which should shift it toward kinase-off output (18, 31). When tested for a serine response in the R^- B^- reporter strain, Tsr-AAAAA (EEEQE) responded to serine, albeit with a very high threshold ($K_{1/2}$, ~700 μM) (Fig. 3A).

In the adaptation-proficient (R^+ B^+) reporter strain, Tsr-AAAAA showed slow recovery of kinase activity following stimulation with a $K_{1/2}$ concentration of serine (Fig. 3B). However, unlike wild-type Tsr, Tsr-AAAAA did not produce a spike in kinase activity upon serine removal (Fig. 3B). The kinase activity spike occurs in the Tsr wild-type response because those receptors undergo a net gain in methyl group modifications during adaptation to the serine stimulus. When serine is subsequently removed, the now-excessive methylation state drives the receptors to high kinase activity, which quickly subsides as the adaptation system reduces receptor modification state to its prestimulus level. The Tsr-AAAAA receptor generated higher kinase activity than wild-type Tsr in the R^+ B^+ host (Fig. 3B), so its lack of a kinase spike response might simply mean that its prestimulus kinase activity is already near the maximum level. However, Tsr-AAAAA also did not undergo much net methylation following a large serine stimulus (Fig. 3C). In hosts that had only one adaptation enzyme, this receptor was a good substrate for both CheB and CheR modifications (Fig. 3C) but evinced no net change in methylation state in a host with both adaptation enzymes (Fig. 3C). We conclude that the all-A control cable produces a strong shift to the kinase-on state and that its output is subject to imperfect adaptational control.

Adaptation properties of Tsr-GGGGG. In the R^- B^- reporter strain, Tsr-GGGGG showed sensitive serine responses, but they were anomalous in several respects (Fig. 3A). First, the kinetics of kinase inhibition and recovery were slow (compare the GGGGG and AAAAA responses in Fig. 3A). Second, saturating serine stimuli inhibited only about half of the available kinase activity in the cells, defined by KCN treatment (Fig. 3A) (18). However, these

TABLE 1 Properties of Tsr synthetic control cable mutants

Tsr protein	Level of expression in UU2610[a]	Value in strain UU2567 (R^- B^-)			Value in strain UU2700 (R^+ B^+)		
		$K_{1/2}$ (μM SER)[b]	Hill coefficient[b]	Kinase activity[c]	$K_{1/2}$ (μM SER)[b]	Hill coefficient[b]	Kinase activity[c]
Wild type	1.00	19 ± 1	17 ± 3	1.00	0.5 ± 0.2	3.0 ± 0.9	0.25
Mutants							
GGGGG variants							
GGGGG	0.70	26 ± 18	1.9 ± 0.8	*1.00*	5.1 ± 0.6	1.6 ± 0.2	*0.40*[d]
+R69E	0.90	NR-ON	NR-ON	*0.70*	NR-ON	NR-ON	*0.90*
+T156K	0.65	NR-ON	NR-ON	*0.45*	NR-ON	NR-ON	*0.25*
EEEQE	0.65	4.2	1.3	*0.95*			
QEEEE	1.00	NR-ON	NR-ON	*0.70*			
QQQEE	1.10	NR-ON	NR-ON	*0.75*			
AAAAA variants							
AAAAA	1.30	NR-ON	NR-ON	*0.75*	7.1 ± 1.8	3.4 ± 1.2	0.65
EEEQE	1.25	670	5.5	0.95			
GIGGG	0.95	20 ± 5	9.8 ± 3.1	0.55	3.0 ± 1.2	3.7 ± 0.6	0.20
AIAAA	0.85	49 ± 3	10 ± 1	0.75	2.5 ± 1.0	2.8 ± 1.0	0.65

[a] Expression level of the mutant protein in strain UU2610 (R^- B^-). Values are rounded to the nearest 0.05 and normalized to that for wild-type Tsr.
[b] Values with error ranges represent averages ± standard deviations of two or more independent FRET-based dose-response experiments (see Materials and Methods for details). Values above 10 were rounded to the nearest whole number. NR-ON, no detectable response to 10 mM serine, but high kinase activity.
[c] Kinase activities are averages of two or more independent FRET-based assays, normalized to the value for wild-type Tsr in strain UU2567 and rounded to the nearest 0.05. Values in italics were determined by FRET changes after KCN treatment. See Materials and Methods for experimental details.
[d] A saturating serine stimulus inhibited 50% of this kinase activity.

appear to be true serine responses, because serine-binding site lesions (R69E or T156K) (33) eliminated them (Fig. 3A and Table 1). In R^+ B^+ hosts, Tsr-GGGGG failed to undergo net methylation in response to a saturating serine stimulus (Fig. 3C), which inhibited about half of the total kinase activity (Table 1), and did not exhibit any behavioral adaptation following a $K_{1/2}$ serine stimulus (Fig. 3B). Tsr-GGGGG also underwent little modification in R^- B^+ and R^+ B^- hosts, a distinct difference from the extensive modification of Tsr-AAAAA in those hosts (Fig. 3C). These severe adaptation and modification defects, in conjunction with inefficient kinase control, probably account for the failure of the all-G control cable to support serine chemotaxis in soft agar assays.

A and G missense mutants of the Tsr control cable. To determine whether a particular control cable residue might be primarily responsible for the anomalous signaling properties of the AAAAA and GGGGG Tsr variants, we examined the behaviors of pRR53 derivatives with single A and G replacements at each Tsr control cable position. Control cable residues 215, 216, and 217 tolerated A and/or G replacements with little change in functionality, as defined by their serine responses, by their adaptation behaviors (see Fig. S1 in the supplemental material), and by chemotaxis assays on semisolid media. Their serine sensitivities were similar to those of wild-type Tsr in both R^- B^- and R^+ B^+ FRET reporter strains (Table 2). Their sensory adaptation rates and modification changes were also similar to those of wild-type Tsr (see Fig. S1). These receptors also mediated robust serine chemotaxis in soft agar assays (12). Tsr-G213A exhibited somewhat ON-shifted responses in both R^- B^- and R^+ B^+ hosts (Table 2), but otherwise its signaling behavior, including its performance in soft agar assays, resembled that of wild-type Tsr (see Fig. S2) (12).

Tsr-I214G and -I214A mutants were distinctly different from wild-type Tsr (Table 2; see also Fig. S2). Both of these I214 mutants had extremely ON-shifted output and could not respond to serine in the R^- B^- background. They showed serine responses in the R^+ B^+ host (Table 2), indicative of some output control by the sensory adaptation system. Of the two mutants, Tsr-I214G had the higher response threshold, both in FRET assays (Table 2) and in minimal soft agar chemotaxis assays (see Fig. S2).

Adaptation behaviors of G213A, I214G, and I214A control cables. In the R^+ B^+ FRET reporter strain, Tsr-G213A exhibited rapid adaptation to a $K_{1/2}$ serine stimulus, but adaptation ceased before full recovery of kinase activity (Fig. 4A). Tsr-I214G and Tsr-I214A produced considerably higher kinase activities in this host background and showed some adaptation to serine stimuli but no evidence of a kinase spike upon serine removal (Fig. 4A). These adaptation behaviors parallel the modification patterns of the mutant receptors (Fig. 4B). Neither Tsr-I214A nor Tsr-I214G exhibited detectable methylation increases following a saturating serine stimulus (Fig. 4B), despite recovering a substantial fraction of initial kinase activity (Fig. 4A).

These results indicate that the G at residue 213 of wild-type Tsr promotes better function than does an A replacement, which causes more ON-shifted response behavior and partially impairs sensory adaptation. However, the aberrant signaling properties of the all-G and all-A synthetic control cables might arise mainly from their G or A replacement at Tsr residue 214. Both mutant amino acids at this control cable position strongly shifted output toward the kinase-on state and both blocked discernible adaptational modifications after a serine stimulus.

Signaling properties of GIGGG and AIAAA synthetic control cables. To determine if the pathological behavior of the all-G and all-A synthetic control cable mutants was mainly due to their amino acid replacements at residue 214, we restored the wild-type isoleucine residue at that position. Both Tsr-GIGGG and Tsr-AIAAA mediated chemotactic migrations in soft agar assays that were indistinguishable from that with the wild type (see Fig. S3 in the supplemental material). In the R^+ B^+ FRET reporter strain, both mutant receptors produced serine responses that were either

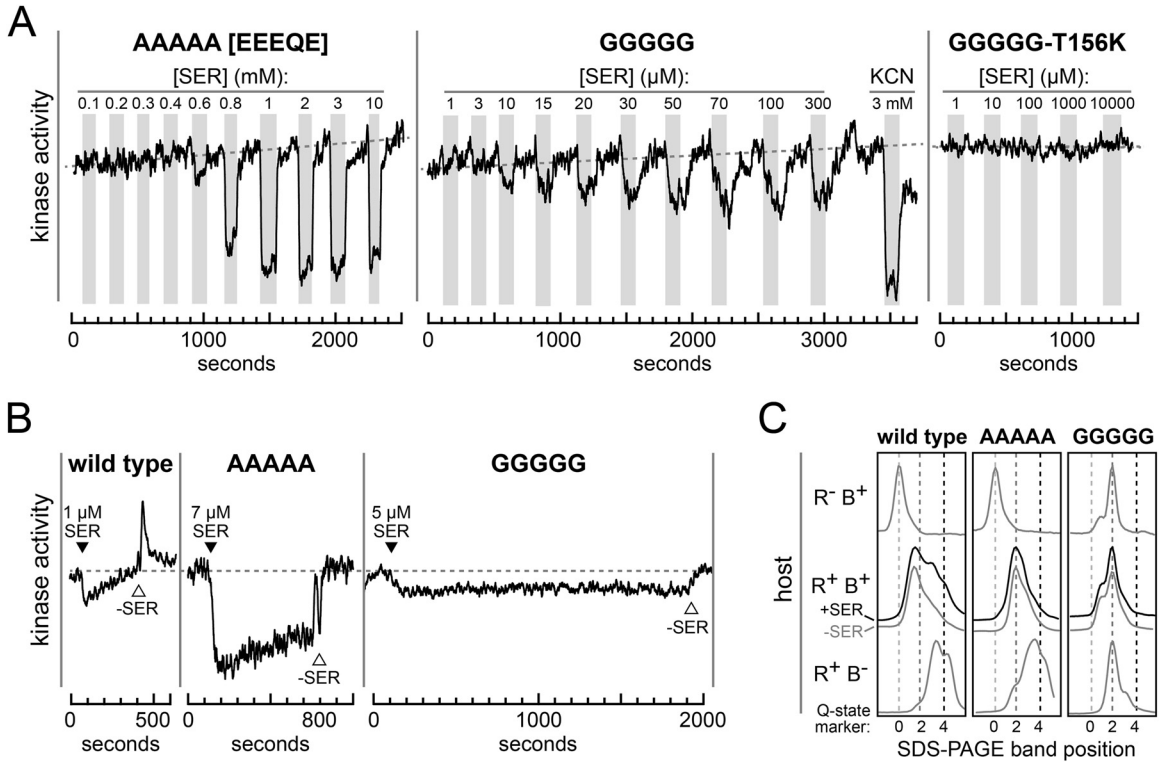

FIG 3 Signaling and adaptation behaviors of Tsr all-A and all-G control cable mutants. (A) Raw data (YFP/CFP) from FRET kinase assays with strain UU2567 (R^- B^-) carrying the indicated pRR53 derivatives. All graphs have the same kinase activity scale. Dashed lines indicate prestimulus kinase activity. Gray bars indicate times when cells were exposed to the indicated serine (SER) or KCN concentrations. Note that the serine concentrations that elicited responses by Tsr-AAAAA (EEEQE) are in millimolar units. (B) Raw data (YFP/CFP) from FRET kinase assays with strain UU2700 (R^+ B^+) carrying the indicated pRR53 derivatives. All graphs have the same kinase activity scale. Black triangles mark the time of addition of the indicated serine concentration; white triangles mark the time of serine removal. The Tsr-GGGGG data were corrected for baseline drift, as described in Materials and Methods. (C) Densitometry traces of SDS-PAGE Western blots of wild-type, all-A, and all-G Tsr variants expressed from plasmid pRR53 in three host strains: UU2611 (R^- B^+), UU2612 (R^+ B^+), and UU2632 (R^+ B^-). Vertical broken lines indicate the band positions of Tsr modification state standards: Q of 0 = EEEEE, Q of 2 = QEQEE, and Q of 4 = QQQQE.

more sensitive (AIAAA) or more cooperative (GIGGG) than those of their all-A and all-G counterparts (Fig. 5A and Table 1). However, the serine response thresholds of the mutant receptors were still higher than that of wild-type Tsr, indicating some residual kinase-on output bias (Fig. 5A and Table 1). Both mutant receptors exhibited rapid, but incomplete, sensory adaptation in response to a $K_{1/2}$ serine stimulus (Fig. 5B). Thus, restoration of an isoleucine at residue 214 corrected many of the signaling defects of the Tsr-AAAAA and Tsr-GGGGG mutant receptors.

In the R^- B^- FRET reporter strain, the AIAAA and GIGGG receptors exhibited $K_{1/2}$ values not greatly different than with the wild type (Fig. 5A). Recall that the all-A control cable was effectively locked in the kinase-on output mode under these conditions. Evidently, having an isoleucine at position 214 in an otherwise all-A control cable conferred a much greater shift toward the kinase-off output state than did a mutationally imposed EEEQE modification state in Tsr-AAAAA (compare Fig. 3A and 5A).

Amino acid replacements at I214 that cause kinase-off output shifts. We previously noted amino acid replacements at residue 214 of Tsr that impaired (I214L, I214N, and I214H) or abrogated (I214R) chemotactic signaling in tryptone soft agar assays (12). The flagellar rotation patterns produced by those mutant receptors indicated that they had off-shifted or "ATT-mimic" outputs (12). We retested the I214H, I214L, I214N, and I214R mutant receptors with the FRET kinase assay to better establish their output shifts, serine thresholds, and sensory adaptation behaviors (Table 3). The L, N, and H replacements shifted Tsr toward the kinase-off state in the R^- B^- reporter strain and further enhanced serine response sensitivity in the adaptation-proficient reporter strain. Tsr-I214R had a more dramatic defect: its output was locked in the kinase-off state in all hosts (Table 3). The modification patterns of these I214 missense proteins by the CheB and CheR sensory adaptation enzymes, characterized in our previous report (12), are summarized in Discussion.

DISCUSSION

Signaling and adaptation properties of Tsr control cable mutants. Figure 6 summarizes the signaling properties of the mutant receptors described in this report. Control cable alterations I214H, I214N, and I214L shifted output toward the kinase-off state; I214A, I214G, and AAAAA shifted output toward the kinase-on state (Fig. 6A). The substrate properties of these mutant receptors for the sensory adaptation enzymes were consistent with their inferred signaling shifts. OFF-shifted receptors were more readily modified by CheR than by CheB, whereas ON-shifted receptors were more readily modified by CheB than by CheR (Fig. 6B). These modification patterns indicate that CheR acts best on OFF-state receptors, whereas CheB preferentially modifies ON-state receptors. Consistent with this scenario, Tsr-I214R, a lock-

TABLE 2 Properties of Tsr A and G missense control cable mutants

Tsr protein	Level of expression in UU2610[a]	Value in strain UU2567 (R^- B^-)			Value in strain UU2700 (R^+ B^+)		
		$K_{1/2}$ (μM SER)[b]	Hill coefficient[b]	Kinase activity[c]	$K_{1/2}$ (μM SER)[b]	Hill coefficient[b]	Kinase activity[c]
Wild type	1.00	19 ± 1	17 ± 3	1.00	0.5 ± 0.2	3.0 ± 0.9	0.25
Mutants							
G213A	0.80	79 ± 2	12 ± 4	0.80	4.1 ± 0.8	8.4 ± 5.2	0.25
I214G	0.75	NR-ON	NR-ON	*1.15*	13 ± 1	8.1 ± 1.3	1.50
I214A	1.15	NR-ON	NR-ON	*1.25*	1.5 ± 0.6	4.2 ± 0.8	1.05
K215G	0.85	37 ± 6	21 ± 10	0.95	0.7 ± 0.1	2.2 ± 1.3	0.30
K215A	1.00	28	7.7	0.80	0.5 ± 0.0	1.5 ± 0.1	0.30
A216G	0.75	24 ± 1	14 ± 2	0.60	0.9 ± 0.1	1.2 ± 0.0	0.30
S217G	1.70	17 ± 0	11 ± 1	0.25	0.6 ± 0.3	1.5 ± 0.5	0.35
S217A	1.15	9.3 ± 0	13 ± 8	0.85	0.7 ± 0.1	1.0 ± 0.1	0.40

[a] Expression level of the mutant protein in strain UU2610 (R^- B^-). Values are rounded to the nearest 0.05 and normalized to that for wild-type Tsr.
[b] Values with error ranges represent averages ± standard deviations of two or more independent FRET-based dose-response experiments (see Materials and Methods for details). Values above 10 were rounded to the nearest whole number. NR-ON, no detectable response to 10 mM serine, but high kinase activity.
[c] Kinase activities are averages of two or more independent FRET-based assays, normalized to the value for wild-type Tsr in strain UU2567. All values are rounded to the nearest 0.05. Values in italics were determined by FRET changes after KCN treatment. See Materials and Methods for experimental details.

OFF mutant receptor, was refractory to CheB but fully modified by CheR (Fig. 6B).

The majority of control cable mutants studied in this work had signaling properties similar to those of wild-type Tsr (Fig. 6A). These receptors were good substrates for both sensory adaptation enzymes (Fig. 6B), but they exhibited some differences in adaptation ability. Five (S217A, S217G, A216G, K215A, and K215G mutants) had wild-type serine sensitivities, both in a host lacking CheR and CheB and in one containing those sensory adaptation enzymes (Fig. 6A). The mutant receptors also exhibited complete adaptation to a $K_{1/2}$ serine stimulus (see Fig. S1 in the supplemental material). In contrast, three mutants (GIGGG, AIAAA, and G213A mutants) had near-normal response sensitivity in the adaptation-deficient host but failed to reach wild-type sensitivity in the adaptation-proficient host (Fig. 6A). Following a $K_{1/2}$ serine stimulus in the adaptation-proficient host, these mutant receptors approached, but did not fully attain, their prestimulus kinase activities (Fig. 4A and 5B). The adaptation shortcomings of these three receptors may arise from slight ON-shifted character but had no discernible impact on their chemotactic performance in soft agar assays.

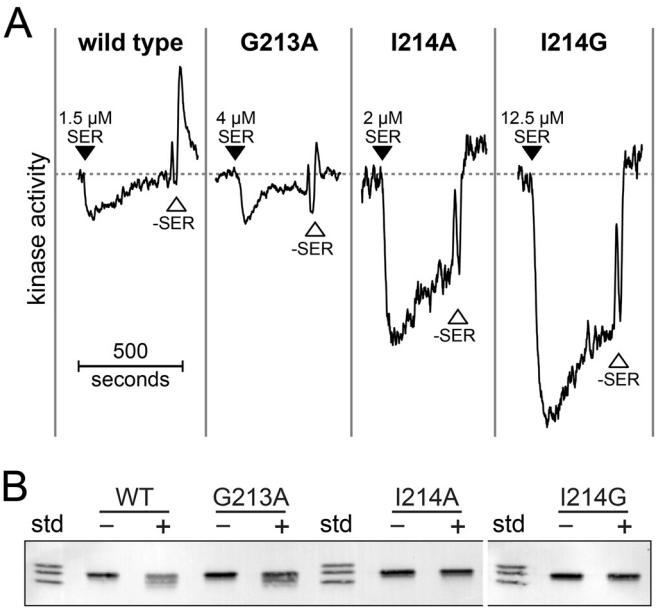

FIG 4 Adaptation and modification properties of Tsr-G213A, -I214G, and -I214A. (A) Raw data (YFP/CFP) from FRET kinase assays with strain UU2700 (R^+ B^+) carrying the indicated pRR53 derivatives. See the legend to Fig. 3B for additional details. Note that kinase activities transiently increase at the time of serine removal due to a brief pump stop, during which the cells metabolize serine in the flow chamber. When pumping resumes, fresh serine-containing solution in the tubing enters the chamber, once again reducing kinase activity, before the serine-free buffer enters the flow cell. (B) SDS-PAGE band patterns of the indicated Tsr proteins, visualized by Western blotting (see Materials and Methods). Three Tsr Q-state variants were run in the "std" lanes as markers (see Fig. 3C). "+" lanes indicate cell samples treated with 1 mM serine; "−" lanes indicate untreated samples. WT, wild type.

In a host containing both adaptation enzymes, the strongly ON-shifted receptors (I214A, I214G, and AAAAA mutants) also mediated chemotactic responses (Fig. 2A; see also Fig. S2 in the supplemental material) but exhibited more aberrant adaptation behaviors (Fig. 3B and 4A). These mutant receptors underwent slow, partial recovery of prestimulus kinase activity that was not accompanied by any discernible net change in modification state (Fig. 3C, 4B, and 6B). However, in hosts that had only one adaptation enzyme, these receptors proved to be good substrates for both CheB and CheR (Fig. 3C and 6B; see also Fig. S4 in the supplemental material). Conceivably, a single CheR or CheB modification converts the receptor to a potent substrate for the alternative enzyme, so that in cells with both enzymes, the mutant receptors cycle rapidly between CheR- and CheB-modified forms with little net change in methylation state.

The mechanism responsible for the partial recovery of kinase activity in ON-shifted receptors, also noted in a previous report (18), is unknown, but it might involve stimulus-induced changes in the network connections that link core signaling units in the receptor array (34).

Evidence for a neutral Tsr-HAMP signaling state. Tsr-G GGGG responded to serine stimuli with near wild-type sensitivity (Fig. 6A) but was a poor substrate for both CheB and CheR modifications (Fig. 6B). Consequently, this mutant receptor did not

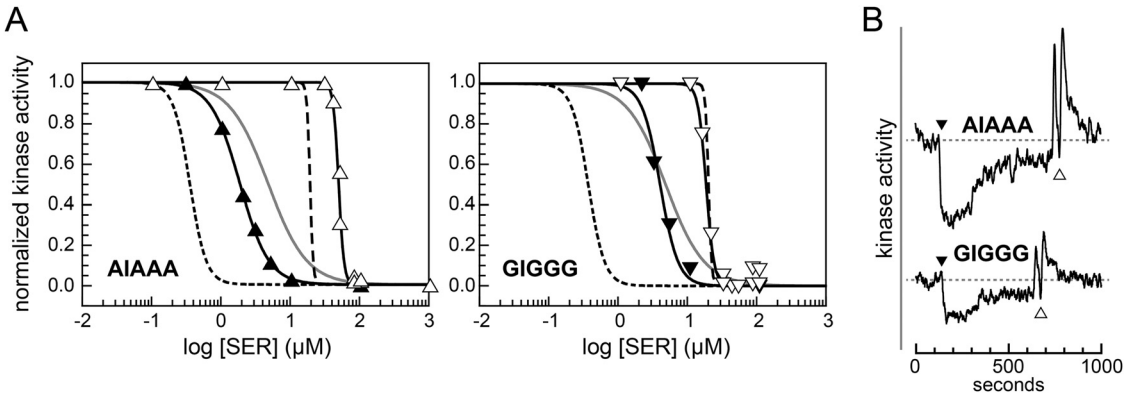

FIG 5 Signaling and adaptation behaviors of Tsr-GIGGG and Tsr-AIAAA. (A) Hill fits of serine dose-response data for pRR53 derivatives in FRET reporter strains UU2567 (R^- B^-) (white symbols) and UU2700 (R^+ B^+) (black symbols). The curves for wild-type Tsr (broken lines) are reproduced from graph one of Fig. 2C for UU2700 (short dashes) and UU2567 (long dashes). Gray lines indicate dose-response curves for the corresponding all-A and all-G variants of Tsr in UU2700, taken from graphs two and three of Fig. 2C, respectively. $K_{1/2}$ and Hill coefficient values in UU2567 and UU2700 for these particular experiments were as follows: Tsr-AIAAA, 49 μM and 11 (white triangles) and 1.8 μM and 2.1 (black triangles); Tsr-GIGGG, 17 μM and 7.5 (white inverted triangles) and 3.8 μM and 3.3 (black inverted triangles). (B) Raw data (YFP/CFP) from FRET kinase assays with strain UU2700 (R^+ B^+) carrying the indicated pRR53 derivatives. Black triangles mark the time of addition of 3 μM serine; white triangles mark the time of serine removal. See the legends to Fig. 3B and 4A for additional details. The GIGGG response data were corrected for baseline drift, as described in Materials and Methods.

undergo sensory adaptation after a serine stimulus (Fig. 3B). These signaling properties of Tsr-GGGGG provide support for the dynamic-bundle model of HAMP action, which posits a series of isoenergetic HAMP conformations along a structural continuum between full-ON and full-OFF signaling states (7) (Fig. 7). The full-ON and full-OFF conformations might resemble the HAMP packing arrangements postulated in the two-state gearbox model (18, 35). We assume that ligand affinity is highest in the full-OFF conformation, allowing a saturating serine stimulus to stabilize that form and drive output to a kinase-off state (Fig. 7). The dynamic-bundle model also proposes that adaptational modifications adjust overall signal output by selectively stabilizing subsets of neighboring conformations along the HAMP continuum. Accordingly, we propose that CheR operates only on receptors in the full-OFF state; its modifications shift output toward the ON state. Similarly, CheB operates only on receptors in the full-ON state; its modifications shift output toward the OFF state (Fig. 7). An isoenergetic conformational landscape should enable wild-type Tsr molecules to populate both conformational extremes and serve as substrates for both adaptation enzymes. Mutant receptors with altered conformational landscapes might not be able to access one or both of these substrate conformations.

We suggest that the all-G control cable destabilizes both the full-ON and full-OFF native HAMP signaling states, thereby confining the receptor to intermediate HAMP conformations that are not effective substrates for either adaptation enzyme (Fig. 7). Tsr-GGGGG produces some kinase activity, but high levels of serine cannot fully inhibit that activity, presumably because the energy barrier to the full-OFF state is too high. Instead, serine drives Tsr-GGGGG to a low kinase-activity conformation that is not a substrate for CheR. Similarly, Tsr-GGGGG seldom enters the full-ON state and is a poor substrate for CheB.

Severe destabilization or ablation of the HAMP domain can also render the Tsr methylation helices impervious to CheR and CheB, but the structural basis for those effects appears to be distinctly different than it is for the Tsr-GGGGG receptor (36). First, Tsr-GGGGG forms kinase-active signaling complexes and partially downregulates their activity in response to serine. In contrast, receptors with HAMP loss-of-function lesions, depending on their severity, may or may not form ternary signaling complexes, but in any case, they cannot regulate kinase activity in response to stimuli (36). Second, Tsr-GGGGG exhibited some modification by CheB (Fig. 3C and 6B), which could account for its slightly enhanced serine response sensitivity in an adaptation-

TABLE 3 Properties of Tsr-I214 missense mutants

Tsr protein	Level of expression in UU2610[a]	Value in host strain[b]			
		UU2567 (R^- B^-)	UU2699 (R^- B^+)	UU2697 (R^+ B^-)	UU2700 (R^+ B^+)
Wild type	1.00	19 ± 1; 17 ± 3	NR-OFF[c]	51; 2.2[d]	0.5 ± 0.2; 3.0 ± 0.9
Mutants					
I214H	1.45	1.2 ± 0.1; 6.6 ± 0.2	NR-OFF	5.8; 2	0.3; 3.6
I214L	1.30	6.9; 24	NR-OFF	15; 2	0.1; 1.6
I214N	1.20	2.5 ± 0; 15 ± 4	NR-OFF	6.1; 1.4	0.2; 1.9
I214R	0.95	NR-OFF	NR-OFF	NR-OFF	NR-OFF

[a] Expression level of the mutant protein in strain UU2610 (R^- B^-) normalized to that of wild-type Tsr and rounded to the nearest 0.05. Data are from reference 12.
[b] Values are means ± standard deviations of $K_{1/2}$ (μM serine) and (after the semicolon) Hill coefficient. Values above 10 were rounded to the nearest whole number.
[c] NR-OFF, no detectable response to 10 mM serine and little or no kinase activity in KCN test.
[d] These values are from reference 18.

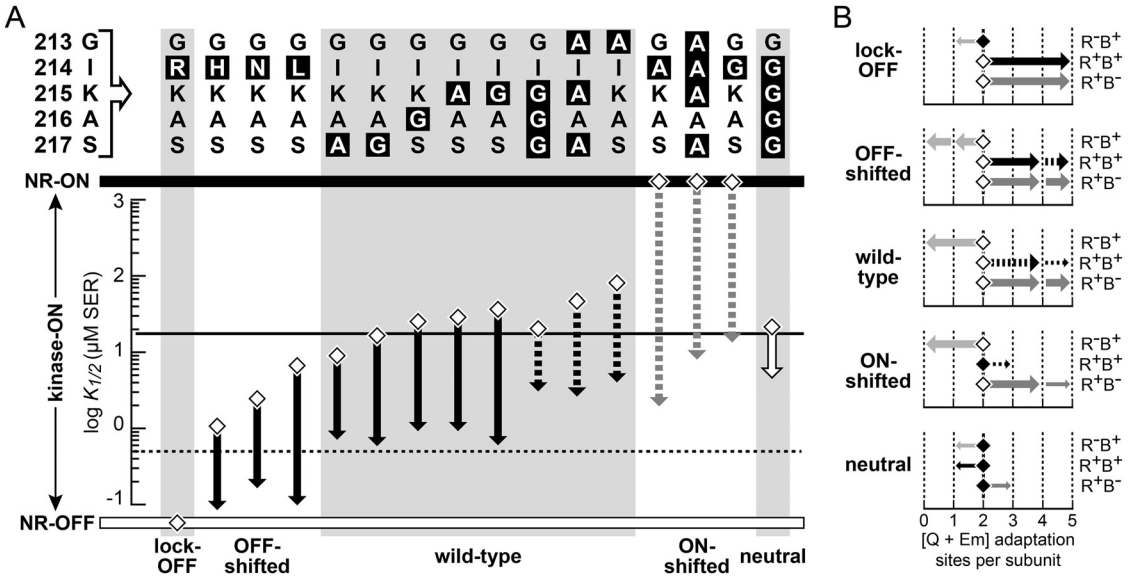

FIG 6 Signaling and adaptational modification properties of Tsr control cable mutants. (A) Serine response sensitivities of cells carrying mutant Tsr plasmids (data from Tables 1, 2, and 3) in host strains UU2567 (R^- B^-; diamonds) and UU2700 (R^+ B^+; arrowheads). Broken black arrows indicate incomplete adaptation to a serine stimulus at the $K_{1/2}$ concentration for that receptor. Broken gray arrows indicate partial, methylation-independent adaptation to a $K_{1/2}$ concentration serine stimulus. The white arrow indicates no discernible adaptation to a $K_{1/2}$ concentration serine stimulus. NR-OFF, no response and no kinase activity; NR-ON, no response and high kinase activity. Horizontal lines indicate the corresponding $K_{1/2}$ values for wild-type Tsr (19 μM in UU2567; ~0.5 μM in UU2700). Phenotypic signaling classes are listed at the bottom. (B) Adaptational modification of receptor subunits in various host strains. This summary is based on SDS-PAGE analyses of mutant Tsr proteins and the mobilities of their methylated forms relative to their Q-state counterparts (see Fig. S4 and S5 in the supplemental material; and data from reference 12). Diamonds indicate the 2-Q (QEQEE) state in UU2610 (R^- B^-). Arrowheads indicate predominant modification states in hosts with one or both adaptation enzymes: R^- B^+ (UU2611; light gray arrows), R^+ B^- (UU2632; dark gray arrows), and R^+ B^+ (UU2612; black arrows). White diamonds indicate that the majority of subunits are shifted from the 2-Q state in a particular host. Black diamonds indicate that the majority of subunits remain at the 2-Q position in a particular host. Thick arrows indicate major-modification species; thin arrows indicate minor extents of modification. Broken arrows indicate modification changes elicited by a saturating serine stimulus.

proficient host (Fig. 2C and 6A). Furthermore, mutational conversion of Tsr-GGGGG from the QEQEE to the EEEQE modification state increased its serine sensitivity in a host lacking the sensory adaptation enzymes (Table 1). Thus, even though the Tsr-GGGGG receptor is a poor substrate for the sensory adaptation enzymes, its modification state can influence its signal output. In contrast, mutationally imposed modification state changes have no effect on the signal outputs of receptors with severe HAMP structural lesions (17, 36). Such loss-of-function lesions drive HAMP into a nonphysiological regime that produces counterintuitive effects on receptor output and adaptation control (Fig. 7) (6, 17, 36).

Other unusual signaling properties of Tsr-GGGGG are consistent with this mechanistic picture. The time courses of kinase inhibition and recovery by Tsr-GGGGG upon serine presentation and removal were notably slow compared to the response kinetics of wild-type and other mutant receptors (Fig. 3A and B). Moreover, Tsr-GGGGG responses were less cooperative than those of other receptors (Fig. 2C). These signaling deficits indicate that the all-G control cable exerts less effective mechanical control over HAMP structure, perhaps because the mutant control cable has reduced helix potential. If that is the case, then the fact that Tsr-GGGGG is unable to reach either the full-ON or full-OFF signaling state implies that control cable helicity contributes to both of those HAMP conformations.

Structural considerations for transmembrane signaling by Tsr. Negative cooperativity at the ligand-binding site ensures that a serine stimulus induces a piston displacement in only one Tsr subunit. However, two lines of evidence indicate that the resultant structural asymmetry is not essential to the transmembrane signaling mechanism. First, the nitrate-sensing domain of NarX, which undergoes quasisymmetric conformational changes upon ligand binding (37), mediates chemotactic responses to nitrate gradients in a chimeric chemoreceptor (38, 39). Second, the control cable alterations in the present study were necessarily present in both subunits of the receptor dimer, presumably creating symmetric conformational changes in the mutant Tsr molecules. The mutant control cables nevertheless mimicked the signaling effects of stimulus inputs, shifting Tsr output toward the kinase-on or kinase-off state. Thus, both asymmetric and symmetric conformational changes in the Tsr control cable can elicit signaling responses, presumably through similar structural effects on HAMP.

The TM2-control cable-AS1 segments in the two subunits of a Tsr molecule most likely act independently, but additively, to modulate the structure or packing stability of the HAMP bundle. The probable distances between the TM2 and TM2′ helices in the TM bundle (4) and between the AS1 and AS1′ helices of the HAMP bundle (40, 41), which together dictate the subunit spacing in the control cable region, preclude significant intersubunit structural interactions between the side chains of control cable residues. Indeed, Tar receptors with cysteine replacements at various control cable positions do not efficiently form intersubunit disulfide bonds (40, 42). It is possible that control cable residues interact with another part of the receptor molecule, but there is as yet no experimental evidence in support of that idea. The nearest potential targets, the N-terminal residues at the cytoplasmic end

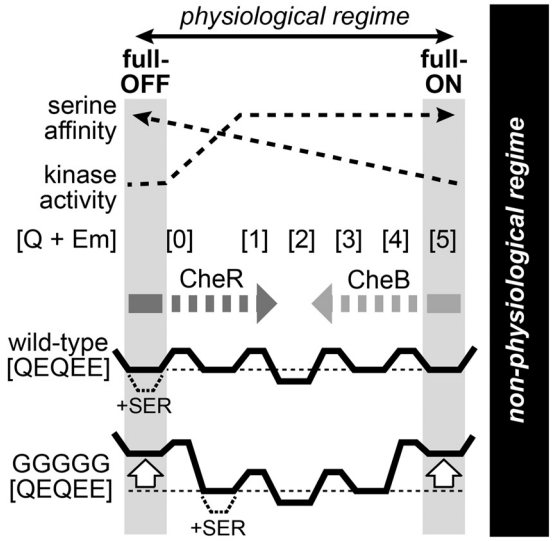

FIG 7 Proposed energy landscapes of the HAMP domains in Tsr wild-type and Tsr-GGGGG receptors. The wild-type HAMP domain may adopt multiple isoenergetic conformations, ranging from a high-kinase-activity, low-serine-affinity state (full-ON) to a low-kinase-activity, high-serine-affinity state (full-OFF) at opposite extremes of the physiological regime. Within this structural range, the dynamic-bundle model specifies that HAMP is most stable in the full-OFF state and least stable in the full-ON state (7). Further destabilization of the HAMP bundle drives the system into a nonphysiological regime that is not relevant to the present study (6, 17, 36). Receptors with HAMP in the full-OFF conformation are proposed to have methylation helices that are substrates for CheR modification; receptors with HAMP in the full-ON conformation are proposed to have methylation helices that are substrates for CheB modification. Each receptor modification state ([Q + Em]) reduces the free energies of a subset of neighboring conformations along this structural continuum. Receptors in low-modification states produce graded kinase outputs; at higher modification states (comparable to 1 to 5 Q sites per subunit), receptors produce high activity levels that are indistinguishable in the FRET kinase assay. The landscapes show energy profiles for wild-type and Tsr-GGGGG receptors in the QEQEE modification state, which favors a conformation intermediate to the full-ON and full-OFF ones. The GGGGG control cable destabilizes both extreme conformations (white arrows), effectively confining the receptor to intermediate conformational states. Thus, serine binding drives wild-type Tsr, but not Tsr-GGGGG, to the full-OFF state (dashed line energy wells).

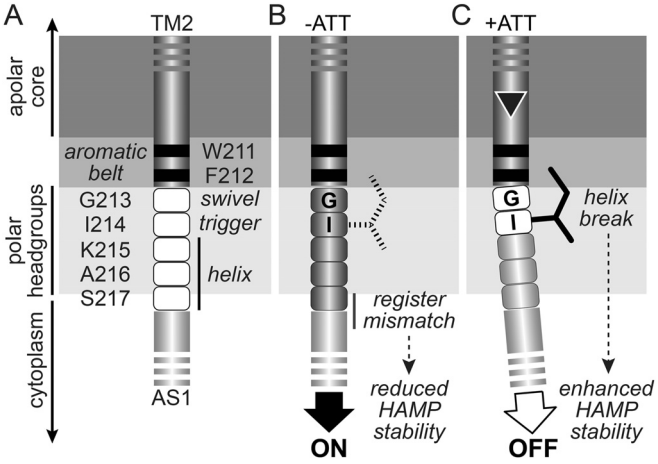

FIG 8 Mechanistic model of transmembrane signaling in Tsr. All panels show residues at the TM2-AS1 junction of one Tsr subunit and the interfacial region of the membrane, shaded from light gray (polar) to dark gray (apolar). This membrane location is based on studies of the TM2 segment in the Trg chemoreceptor (45). Similar experiments with Tar-TM2 (46) suggested that the second and third control cable residues in that receptor might lie within the transition zone between the apolar core and polar headgroups. (A) Signaling roles of control cable residues (white fill). The C terminus of TM2 and the N terminus of AS1 are assumed to be α-helices (dark gray and light gray cylinders, respectively). Three of the control cable residues (K215, A216, and S217) are proposed to favor an α-helical secondary structure in both signaling states, whereas stimulus input modulates the helix potential of G213 and I214. (B) The ON state. All five residues of the control cable adopt a helical secondary structure, which propagates the TM2 helix register toward AS1 and destabilizes the HAMP bundle. The I214 side chain (broken lines) plays no critical structural role in this signaling state. (C) The OFF state. Inward piston displacement (triangle) of TM2 induces a break or kink at G213 of the control cable, alleviating the register mismatch between the TM2 and AS1 helices and stabilizing the HAMP bundle. Interaction of the I214 side chain with the membrane interfacial region promotes this structural change.

of TM1, are not critical for function in Tar (43). Moreover, only one control cable residue in Tsr, I214, is critical for transmembrane signaling, which implies that the other control cable positions do not engage in specific side chain interactions with residues elsewhere in the protein.

Helix-destabilizing proline or multiple glycine replacements in the control cable impair transmembrane signaling in both Tsr (12) and Tar (11). Moreover, the signaling properties of Tsr-GGGGG indicate that both the full-OFF and full-ON output states depend on the control cable having helix character. If the 5-residue control cable has α-helical secondary structure, then the preferred orientations of the flanking TM2 and AS1 helices would be ~140° out of register, as first noted by Swain and Falke (41). The structural mismatch between the TM2 and AS1 helix registers could provide the mechanistic key for transmembrane signal control in chemoreceptors.

A mechanistic model of transmembrane signaling by Tsr. We present our mechanistic ideas in the context of the dynamic-bundle model of HAMP signaling, but the central principles of our model (Fig. 8) are also consistent with discrete two-state conformational views of HAMP signaling, such as the gearbox model. We propose that in kinase-on output states, the TM2-control cable segment is a continuous α-helix. The helical structure of the control cable connection maximizes the register mismatch between TM2 and AS1, thereby destabilizing HAMP bundle packing (Fig. 8B). In kinase-off output state, a structural change at the beginning of the control cable helix reduces or alleviates the TM2-AS1 register mismatch, allowing the HAMP bundle to adopt a more stable packing arrangement. The control cable residues nearest AS1 might retain their helical character, thereby augmenting AS1 helicity and further enhancing HAMP packing stability (Fig. 8C).

We propose that an inward TM2 piston displacement promotes kinase-off output by modulating the continuity of the control cable helix. The first two control cable residues are identical in Tsr (G213 and I214) and Tar (G211 and I212) and play important roles in that structural transition. The glycine residue, lacking a side chain, might serve as a structural swivel or flexion site in the control cable helix. The isoleucine residue might trigger or stabilize the helix discontinuity through interaction of its branched hydrophobic side chain with a nonpolar region of the membrane. As shown in this work, the isoleucine position is the more critical residue in Tsr, whereas the glycine position is the more critical residue in Tar (44). The precise structural environments of these key residues are presumably responsible for these differences.

The Tsr control cable most likely resides in the polar headgroup region at the membrane-cytoplasm interface, with residue 214 close to the transition zone between the charged headgroups and the apolar core (Fig. 8A) (45). The distal end of the hydrophobic I214 side chain might partition into that nonpolar region (Fig. 8B and C). That structural interaction could be the basis for signal transmission through the control cable. It presumably plays no active role in promoting kinase-on output, because G and A replacements at residue 214 produce strongly ON-shifted output (Fig. 8B). Rather, I214 actively enables the receptor to attain a kinase-off output state. Leucine can evidently play a similar, but stronger, role at the 214 position: the signaling behavior of Tsr-I214L was considerably OFF-shifted relative to that of wild-type Tsr. Unlike that of isoleucine, the leucine side chain has branched methyl groups at its distal end, which might enhance its interaction with the nonpolar membrane region.

Attractant-induced TM2 piston motions could exploit the I214 side chain interaction in several ways to initiate or stabilize a structural change in the control cable helix. (i) The I214 interaction could oppose TM2 displacements that attempt to push the critical G213 and I214 control cable residues further into the headgroup region. In conjunction with rotational freedom at G213, the structural stress might create a bend or kink in the control cable helix that alleviates the HAMP-destabilizing register mismatch. (ii) Alternatively, I214 and the TM2 aromatic belt residues, W211 and F212, which also partition at the core-headgroup interface (46, 47) (Fig. 8C), could constrain the cytoplasmic end of TM2 to lateral movements in the membrane. Thus, piston motions might produce a slight bend in the TM2 helix (14), which could modulate HAMP stability by altering the alignment and helix strength of the TM2-control cable-AS1 segment.

In summary, a side chain interaction between residue I214 and the local membrane environment appears to be necessary and sufficient for proper transmembrane signaling by the Tsr control cable. The aberrant signaling behavior of Tsr-GGGGG and Tsr-AAAAA receptors is almost entirely caused by their I214 replacements: Tsr-GIGGG and Tsr-AIAAA exhibited near-normal signaling properties in adaptation-competent cells. Residue G213 of the control cable plays a subsidiary role but is much less critical in Tsr than in Tar; many other amino acids at that position also support transmembrane signaling in Tsr (12). Residues 215, 216, and 217 of the Tsr control cable tolerate a variety of amino acid replacements with no evident effect on signaling function. Our working model predicts that in addition to the key role of residue I214, the length of the control cable should also be a critical factor for transmembrane signaling because the number of control cable residues will set the force of the register mismatch mechanism. Removal of one residue should alleviate much of the HAMP-destabilizing structural input; addition of one residue should exacerbate HAMP instability. Our current work on transmembrane signaling in Tsr aims to test these mechanistic predictions.

ACKNOWLEDGMENTS

Thanks go to David Blair (University of Utah) for helpful discussions during this study.

This work was supported by research grant GM19559 from the National Institute of General Medical Sciences. The Protein-DNA Core Facility at the University of Utah receives support from National Cancer Institute grant CA42014 to the Huntsman Cancer Institute.

REFERENCES

1. **Parkinson JS, Hazelbauer GL, Falke JJ.** 2015. Signaling and sensory adaptation in Escherichia coli chemoreceptors: 2015 update. Trends Microbiol **23:**257–266. http://dx.doi.org/10.1016/j.tim.2015.03.003.
2. **Yu D, Ma X, Tu Y, Lai L.** 2015. Both piston-like and rotational motions are present in bacterial chemoreceptor signaling. Sci Rep **5:**8640. http://dx.doi.org/10.1038/srep08640.
3. **Chervitz SA, Falke JJ.** 1996. Molecular mechanism of transmembrane signaling by the aspartate receptor: a model. Proc Natl Acad Sci U S A **93:**2545–2550. http://dx.doi.org/10.1073/pnas.93.6.2545.
4. **Falke JJ, Hazelbauer GL.** 2001. Transmembrane signaling in bacterial chemoreceptors. Trends Biochem Sci **26:**257–265. http://dx.doi.org/10.1016/S0968-0004(00)01770-9.
5. **Ottemann KM, Xiao W, Shin YK, Koshland DE, Jr.** 1999. A piston model for transmembrane signaling of the aspartate receptor. Science **285:**1751–1754. http://dx.doi.org/10.1126/science.285.5434.1751.
6. **Parkinson JS.** 2010. Signaling mechanisms of HAMP domains in chemoreceptors and sensor kinases. Annu Rev Microbiol **64:**101–122. http://dx.doi.org/10.1146/annurev.micro.112408.134215.
7. **Zhou Q, Ames P, Parkinson JS.** 2009. Mutational analyses of HAMP helices suggest a dynamic bundle model of input-output signalling in chemoreceptors. Mol Microbiol **73:**801–814. http://dx.doi.org/10.1111/j.1365-2958.2009.06819.x.
8. **Swain KE, Gonzalez MA, Falke JJ.** 2009. Engineered socket study of signaling through a four-helix bundle: evidence for a yin-yang mechanism in the kinase control module of the aspartate receptor. Biochemistry **48:**9266–9277. http://dx.doi.org/10.1021/bi901020d.
9. **Coleman MD, Bass RB, Mehan RS, Falke JJ.** 2005. Conserved glycine residues in the cytoplasmic domain of the aspartate receptor play essential roles in kinase coupling and on-off switching. Biochemistry **44:**7687–7695. http://dx.doi.org/10.1021/bi0501479.
10. **Alexander RP, Zhulin IB.** 2007. Evolutionary genomics reveals conserved structural determinants of signaling and adaptation in microbial chemoreceptors. Proc Natl Acad Sci U S A **104:**2885–2890. http://dx.doi.org/10.1073/pnas.0609359104.
11. **Wright GA, Crowder RL, Draheim RR, Manson MD.** 2011. Mutational analysis of the transmembrane helix 2-HAMP domain connection in the *Escherichia coli* aspartate chemoreceptor Tar. J Bacteriol **193:**82–90. http://dx.doi.org/10.1128/JB.00953-10.
12. **Kitanovic S, Ames P, Parkinson JS.** 2011. Mutational analysis of the control cable that mediates transmembrane signaling in the *E. coli* serine chemoreceptor. J Bacteriol **193:**5062–5072. http://dx.doi.org/10.1128/JB.05683-11.
13. **Hall BA, Armitage JP, Sansom MS.** 2011. Transmembrane helix dynamics of bacterial chemoreceptors supports a piston model of signalling. PLoS Comput Biol **7:**e1002204. http://dx.doi.org/10.1371/journal.pcbi.1002204.
14. **Park H, Im W, Seok C.** 2011. Transmembrane signaling of chemotaxis receptor Tar: insights from molecular dynamics simulation studies. Biophys J **100:**2955–2963. http://dx.doi.org/10.1016/j.bpj.2011.05.030.
15. **Parkinson JS, Houts SE.** 1982. Isolation and behavior of *Escherichia coli* deletion mutants lacking chemotaxis functions. J Bacteriol **151:**106–113.
16. **Ames P, Studdert CA, Reiser RH, Parkinson JS.** 2002. Collaborative signaling by mixed chemoreceptor teams in *Escherichia coli*. Proc Natl Acad Sci U S A **99:**7060–7065. http://dx.doi.org/10.1073/pnas.092071899.
17. **Zhou Q, Ames P, Parkinson JS.** 2011. Biphasic control logic of HAMP domain signalling in the *Escherichia coli* serine chemoreceptor. Mol Microbiol **80:**596–611. http://dx.doi.org/10.1111/j.1365-2958.2011.07577.x.
18. **Lai RZ, Parkinson JS.** 2014. Functional suppression of HAMP domain signaling defects in the *E. coli* serine chemoreceptor. J Mol Biol **426:**3642–3655. http://dx.doi.org/10.1016/j.jmb.2014.08.003.
19. **Chang ACY, Cohen SN.** 1978. Construction and characterization of amplifiable multicopy DNA cloning vehicles derived from the p15A cryptic miniplasmid. J Bacteriol **134:**1141–1156.
20. **Gosink KK, Buron-Barral M, Parkinson JS.** 2006. Signaling interactions between the aerotaxis transducer Aer and heterologous chemoreceptors in *Escherichia coli*. J Bacteriol **188:**3487–3493. http://dx.doi.org/10.1128/JB.188.10.3487-3493.2006.
21. **Bolivar F, Rodriguez R, Greene PJ, Betlach MC, Heyneker HL, Boyer HW.** 1977. Construction and characterization of new cloning vehicles. Gene **2:**95–113. http://dx.doi.org/10.1016/0378-1119(77)90000-2.
22. **Studdert CA, Parkinson JS.** 2005. Insights into the organization and

dynamics of bacterial chemoreceptor clusters through *in vivo* crosslinking studies. Proc Natl Acad Sci U S A **102:**15623–15628. http://dx.doi.org/10.1073/pnas.0506040102.
23. **Sourjik V, Vaknin A, Shimizu TS, Berg HC.** 2007. In vivo measurement by FRET of pathway activity in bacterial chemotaxis. Methods Enzymol **423:**365–391. http://dx.doi.org/10.1016/S0076-6879(07)23017-4.
24. **Parkinson JS.** 1976. *cheA*, che*B*, and *cheC* genes of *Escherichia coli* and their role in chemotaxis. J Bacteriol **126:**758–770.
25. **Laemmli UK.** 1970. Cleavage of structural proteins during the assembly of the head of bacteriophage T4. Nature **227:**680–685. http://dx.doi.org/10.1038/227680a0.
26. **Ames P, Parkinson JS.** 1994. Constitutively signaling fragments of Tsr, the *Escherichia coli* serine chemoreceptor. J Bacteriol **176:**6340–6348.
27. **Berg HC, Block SM.** 1984. A miniature flow cell designed for rapid exchange of media under high-power microscope objectives. J Gen Microbiol **130:**2915–2920.
28. **Sourjik V, Berg HC.** 2002. Receptor sensitivity in bacterial chemotaxis. Proc Natl Acad Sci U S A **99:**123–127. http://dx.doi.org/10.1073/pnas.011589998.
29. **Meir Y, Jakovljevic V, Oleksiuk O, Sourjik V, Wingreen NS.** 2010. Precision and kinetics of adaptation in bacterial chemotaxis. Biophys J **99:**2766–2774. http://dx.doi.org/10.1016/j.bpj.2010.08.051.
30. **Sourjik V, Berg HC.** 2004. Functional interactions between receptors in bacterial chemotaxis. Nature **428:**437–441. http://dx.doi.org/10.1038/nature02406.
31. **Han XS, Parkinson JS.** 2014. An unorthodox sensory adaptation site in the *Escherichia coli* serine chemoreceptor. J Bacteriol **196:**641–649. http://dx.doi.org/10.1128/JB.01164-13.
32. **Shimizu TS, Tu Y, Berg HC.** 2010. A modular gradient-sensing network for chemotaxis in *Escherichia coli* revealed by responses to time-varying stimuli. Mol Syst Biol **6:**382. http://dx.doi.org/10.1038/msb.2010.37.
33. **Ames P, Zhou Q, Parkinson JS.** 2008. Mutational analysis of the connector segment in the HAMP domain of Tsr, the *Escherichia coli* serine chemoreceptor. J Bacteriol **190:**6676–6685. http://dx.doi.org/10.1128/JB.00750-08.
34. **Frank V, Vaknin A.** 2013. Prolonged stimuli alter the bacterial chemosensory clusters. Mol Microbiol **88:**634–644. http://dx.doi.org/10.1111/mmi.12215.
35. **Hulko M, Berndt F, Gruber M, Linder JU, Truffault V, Schultz A, Martin J, Schultz JE, Lupas AN, Coles M.** 2006. The HAMP domain structure implies helix rotation in transmembrane signaling. Cell **126:**929–940. http://dx.doi.org/10.1016/j.cell.2006.06.058.
36. **Ames P, Zhou Q, Parkinson JS.** 2014. HAMP domain structural determinants for signalling and sensory adaptation in Tsr, the *Escherichia coli* serine chemoreceptor. Mol Microbiol **91:**875–886. http://dx.doi.org/10.1111/mmi.12443.
37. **Cheung J, Hendrickson WA.** 2009. Structural analysis of ligand stimulation of the histidine kinase NarX. Structure **17:**190–201. http://dx.doi.org/10.1016/j.str.2008.12.013.
38. **Ward SM, Bormans AF, Manson MD.** 2006. Mutationally altered signal output in the Nart (NarX-Tar) hybrid chemoreceptor. J Bacteriol **188:**3944–3951. http://dx.doi.org/10.1128/JB.00117-06.
39. **Ward SM, Delgado A, Gunsalus RP, Manson MD.** 2002. A NarX-Tar chimera mediates repellent chemotaxis to nitrate and nitrite. Mol Microbiol **44:**709–719. http://dx.doi.org/10.1046/j.1365-2958.2002.02902.x.
40. **Butler SL, Falke JJ.** 1998. Cysteine and disulfide scanning reveals two amphiphilic helices in the linker region of the aspartate chemoreceptor. Biochemistry **37:**10746–10756. http://dx.doi.org/10.1021/bi980607g.
41. **Swain KE, Falke JJ.** 2007. Structure of the conserved HAMP domain in an intact, membrane-bound chemoreceptor: a disulfide mapping study. Biochemistry **46:**13684–13695. http://dx.doi.org/10.1021/bi701832b.
42. **Pakula AA, Simon MI.** 1992. Determination of transmembrane protein structure by disulfide cross-linking: the *Escherichia coli* Tar receptor. Proc Natl Acad Sci U S A **89:**4144–4148. http://dx.doi.org/10.1073/pnas.89.9.4144.
43. **Chen XM, Koshland DE.** 1995. The N-terminal cytoplasmic tail of the aspartate receptor is not essential in signal transduction of bacterial chemotaxis. J Biol Chem **270:**24038–24042. http://dx.doi.org/10.1074/jbc.270.41.24038.
44. **Adase CA, Draheim RR, Rueda G, Desai R, Manson MD.** 2013. Residues at the cytoplasmic end of transmembrane helix 2 determine the signal output of the TarEc chemoreceptor. Biochemistry **52:**2729–2738. http://dx.doi.org/10.1021/bi4002002.
45. **Boldog T, Hazelbauer GL.** 2004. Accessibility of introduced cysteines in chemoreceptor transmembrane helices reveals boundaries interior to bracketing charged residues. Protein Sci **13:**1466–1475. http://dx.doi.org/10.1110/ps.04648604.
46. **Miller AS, Falke JJ.** 2004. Side chains at the membrane-water interface modulate the signaling state of a transmembrane receptor. Biochemistry **43:**1763–1770. http://dx.doi.org/10.1021/bi0360206.
47. **Draheim RR, Bormans AF, Lai RZ, Manson MD.** 2005. Tryptophan residues flanking the second transmembrane helix (TM2) set the signaling state of the Tar chemoreceptor. Biochemistry **44:**1268–1277. http://dx.doi.org/10.1021/bi048969d.

Fig. S1. Sensory adaptation profiles of Tsr control cable mutants.

Plasmids expressing the indicated mutant forms of Tsr were analyzed in FRET reporter strain UU2700 (R^+ B^+). Traces show the YFP/CFP ratio over the course of serine addition at the $K_{1/2}$ concentration previously determined for that receptor (black triangles) and subsequent serine removal (white triangles).

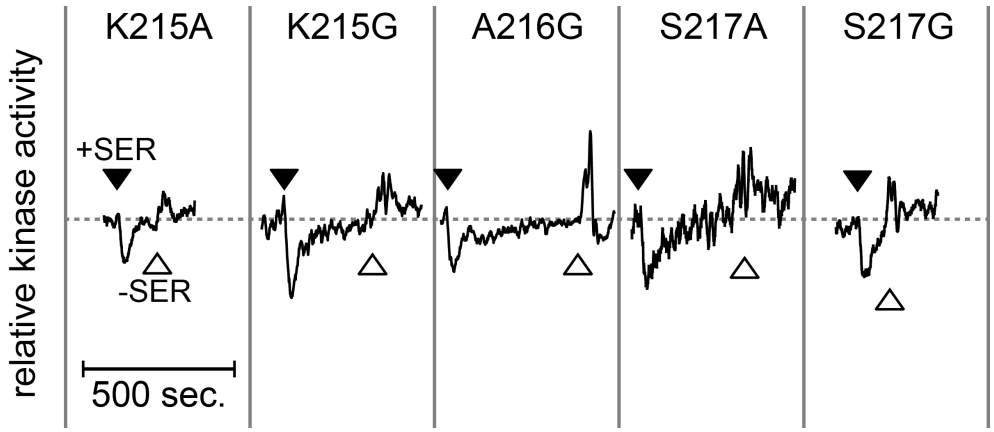

Fig. S2. Chemotaxis phenotypes of Tsr control cable mutants.

Plasmids expressing the indicated mutant forms of Tsr were analyzed in strain UU2612 (R^+ B^+). Plates were photographed after incubation at 30°C for 18 hours.

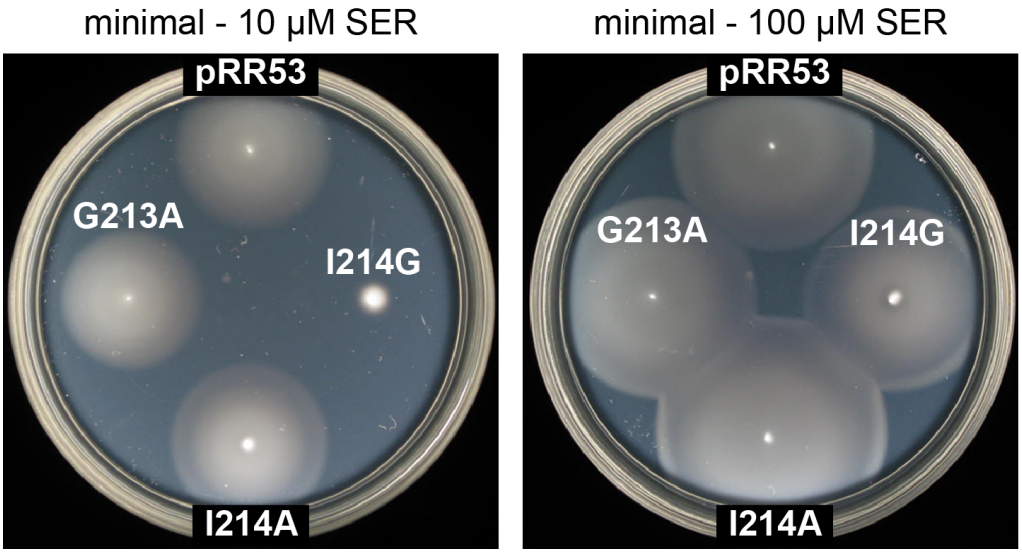

Fig. S3. Chemotaxis phenotypes of Tsr control cable mutants.

Plasmids expressing the indicated mutant forms of Tsr were analyzed in strain UU2612 (R^+ B^+). Plates were photographed after incubation at 30°C for 18 hours.

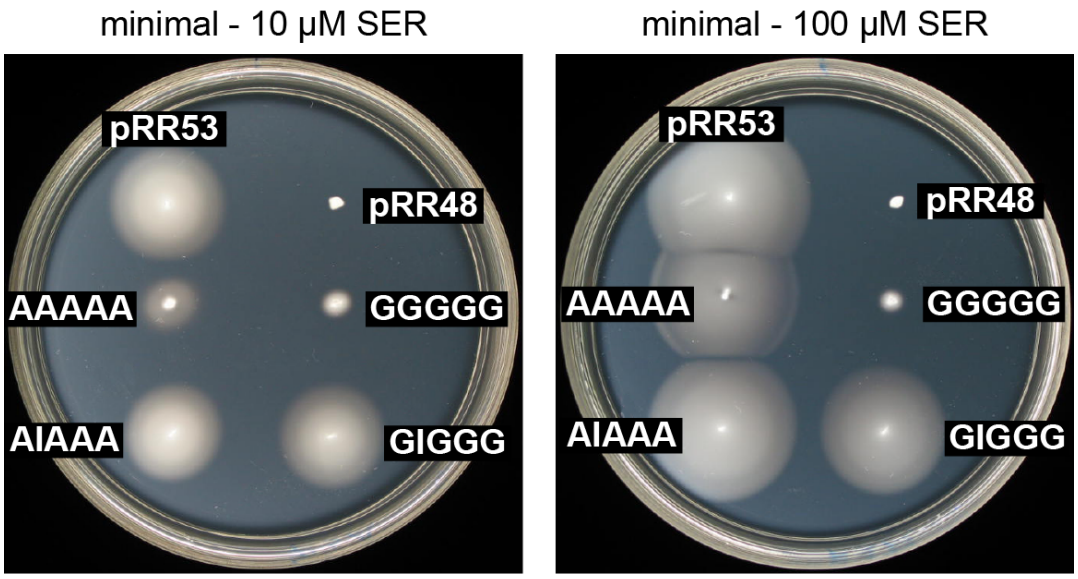

Fig. S4. Modification patterns of Tsr control cable mutants.

Plasmids expressing the indicated mutant forms of Tsr were transferred to strains UU2610 (R^- B^-), UU2611 (R^- B^+) and UU2632 (R^+ B^-). Protein extracts were prepared and analyzed by SDS-PAGE and Tsr bands visualized by western blotting as detailed in Methods. Unlabeled lanes contained a mixture of three Tsr modification states as mobility standards: upper band = Tsr [EEEEE]; middle band = Tsr [QEQEE]; lower band = Tsr [QQQQE].

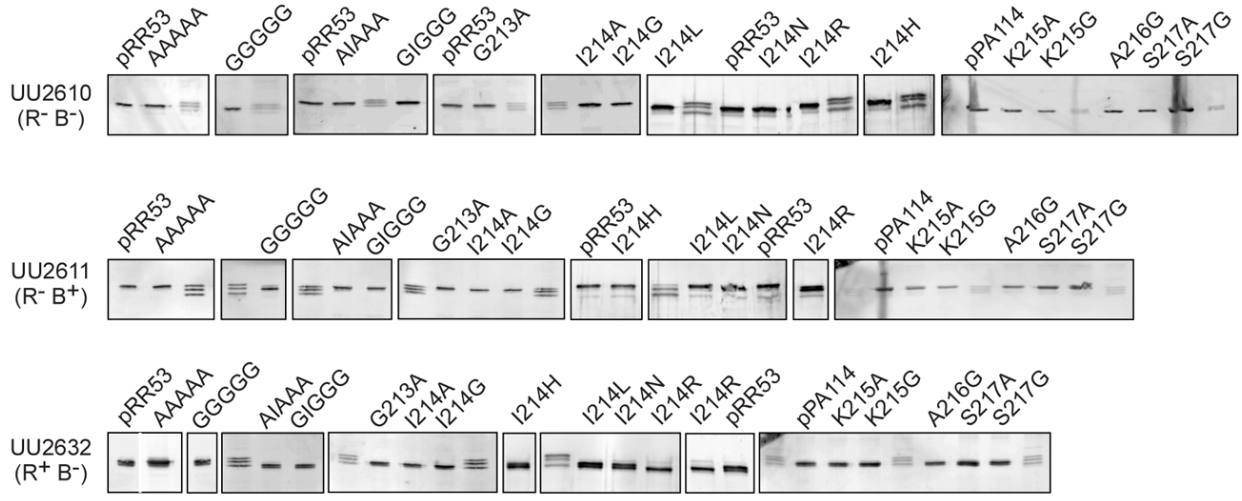

Fig. S5. Modification patterns of Tsr control cable mutants.

Plasmids expressing the indicated mutant forms of Tsr were transferred to strain UU2612 (R^+ B^+). Cells were exposed (+ lanes) or not (- lanes) to serine before preparing the protein extracts. Tsr proteins were analyzed by SDS-PAGE and visualized by western blotting as detailed in Methods. Unlabeled lanes contained a mixture of three Tsr modification states as mobility standards: upper band = Tsr [EEEEE]; middle band = Tsr [QEQEE]; lower band = Tsr [QQQQE].